

Observation of $B^0 \rightarrow D^+ D^-$, $B^- \rightarrow D^0 D^-$ and $B^- \rightarrow D^0 D^{*-}$ decays

G. Majumder,³⁶ K. Abe,⁶ K. Abe,³⁸ I. Adachi,⁶ H. Aihara,⁴⁰ Y. Asano,⁴⁴ V. Aulchenko,¹ T. Aushev,¹⁰ S. Bahinipati,⁴ A. M. Bakich,³⁵ S. Banerjee,³⁶ I. Bedny,¹ U. Bitenc,¹¹ I. Bizjak,¹¹ S. Blyth,²³ A. Bondar,¹ A. Bozek,²⁴ M. Bračko,^{6, 17, 11} J. Brodzicka,²⁴ T. E. Browder,⁵ M.-C. Chang,²³ P. Chang,²³ Y. Chao,²³ A. Chen,²¹ K.-F. Chen,²³ W. T. Chen,²¹ B. G. Cheon,³ R. Chistov,¹⁰ Y. Choi,³⁴ A. Chuvikov,⁴⁷ S. Cole,³⁵ J. Dalseno,¹⁸ M. Danilov,¹⁰ M. Dash,⁴⁵ A. Drutskoy,⁴ S. Eidelman,¹ Y. Enari,¹⁹ S. Fratina,¹¹ N. Gabyshev,¹ T. Gershon,⁶ A. Go,²¹ G. Gokhroo,³⁶ B. Golob,^{16, 11} A. Gorišek,¹¹ J. Haba,⁶ T. Hara,²⁸ N. C. Hastings,⁶ K. Hayasaka,¹⁹ H. Hayashii,²⁰ M. Hazumi,⁶ L. Hinz,¹⁵ T. Hokuue,¹⁹ Y. Hoshi,³⁸ S. Hou,²¹ W.-S. Hou,²³ Y. B. Hsiung,²³ T. Iijima,¹⁹ A. Imoto,²⁰ K. Inami,¹⁹ A. Ishikawa,⁶ R. Itoh,⁶ M. Iwasaki,⁴⁰ J. H. Kang,⁴⁶ J. S. Kang,¹³ N. Katayama,⁶ H. Kawai,² T. Kawasaki,²⁶ H. R. Khan,⁴¹ H. Kichimi,⁶ H. J. Kim,¹⁴ S. K. Kim,³³ S. M. Kim,³⁴ P. Križan,^{16, 11} P. Krokovny,¹ R. Kulásík,⁴ S. Kumar,²⁹ C. C. Kuo,²¹ A. Kuzmin,¹ Y.-J. Kwon,⁴⁶ G. Leder,⁹ S. E. Lee,³³ T. Lesiak,²⁴ J. Li,³² S.-W. Lin,²³ D. Liventsev,¹⁰ J. MacNaughton,⁹ F. Mandl,⁹ T. Matsumoto,⁴² A. Matyja,²⁴ Y. Mikami,³⁹ W. Mitaroff,⁹ K. Miyabayashi,²⁰ H. Miyake,²⁸ H. Miyata,²⁶ R. Mizuk,¹⁰ D. Mohapatra,⁴⁵ G. R. Moloney,¹⁸ T. Nagamine,³⁹ Y. Nagasaka,⁷ I. Nakamura,⁶ E. Nakano,²⁷ M. Nakao,⁶ H. Nakazawa,⁶ Z. Natkaniec,²⁴ S. Nishida,⁶ O. Nitoh,⁴³ S. Ogawa,³⁷ T. Ohshima,¹⁹ T. Okabe,¹⁹ S. Okuno,¹² S. L. Olsen,⁵ W. Ostrowicz,²⁴ H. Ozaki,⁶ H. Palka,²⁴ C. W. Park,³⁴ H. Park,¹⁴ N. Parslow,³⁵ L. S. Peak,³⁵ R. Pestotnik,¹¹ L. E. Piilonen,⁴⁵ M. Rozanska,²⁴ H. Sagawa,⁶ Y. Sakai,⁶ N. Sato,¹⁹ T. Schietinger,¹⁵ O. Schneider,¹⁵ P. Schönmeier,³⁹ J. Schümann,²³ M. E. Sevior,¹⁸ H. Shibuya,³⁷ B. Shwartz,¹ V. Sidorov,¹ J. B. Singh,²⁹ A. Somov,⁴ N. Soni,²⁹ R. Stamen,⁶ S. Stanič,^{44,*} M. Starič,¹¹ K. Sumisawa,²⁸ T. Sumiyoshi,⁴² S. Suzuki,³¹ S. Y. Suzuki,⁶ O. Tajima,⁶ F. Takasaki,⁶ K. Tamai,⁶ N. Tamura,²⁶ M. Tanaka,⁶ G. N. Taylor,¹⁸ Y. Teramoto,²⁷ X. C. Tian,³⁰ T. Tsukamoto,⁶ S. Uehara,⁶ T. Uglov,¹⁰ K. Ueno,²³ S. Uno,⁶ P. Urquijo,¹⁸ G. Varner,⁵ K. E. Varvell,³⁵ S. Villa,¹⁵ C. C. Wang,²³ C. H. Wang,²² M.-Z. Wang,²³ Y. Watanabe,⁴¹ Q. L. Xie,⁸ A. Yamaguchi,³⁹ Y. Yamashita,²⁵ M. Yamauchi,⁶ Heyoung Yang,³³ J. Ying,³⁰ C. C. Zhang,⁸ L. M. Zhang,³² Z. P. Zhang,³² V. Zhilich,¹ and D. Žontar^{16, 11}

(The Belle Collaboration)

¹Budker Institute of Nuclear Physics, Novosibirsk

²Chiba University, Chiba

³Chonnam National University, Kwangju

⁴University of Cincinnati, Cincinnati, Ohio 45221

⁵University of Hawaii, Honolulu, Hawaii 96822

⁶High Energy Accelerator Research Organization (KEK), Tsukuba

⁷Hiroshima Institute of Technology, Hiroshima

⁸Institute of High Energy Physics, Chinese Academy of Sciences, Beijing

⁹*Institute of High Energy Physics, Vienna*

¹⁰*Institute for Theoretical and Experimental Physics, Moscow*

¹¹*J. Stefan Institute, Ljubljana*

¹²*Kanagawa University, Yokohama*

¹³*Korea University, Seoul*

¹⁴*Kyungpook National University, Taegu*

¹⁵*Swiss Federal Institute of Technology of Lausanne, EPFL, Lausanne*

¹⁶*University of Ljubljana, Ljubljana*

¹⁷*University of Maribor, Maribor*

¹⁸*University of Melbourne, Victoria*

¹⁹*Nagoya University, Nagoya*

²⁰*Nara Women's University, Nara*

²¹*National Central University, Chung-li*

²²*National United University, Miao Li*

²³*Department of Physics, National Taiwan University, Taipei*

²⁴*H. Niewodniczanski Institute of Nuclear Physics, Krakow*

²⁵*Nihon Dental College, Niigata*

²⁶*Niigata University, Niigata*

²⁷*Osaka City University, Osaka*

²⁸*Osaka University, Osaka*

²⁹*Panjab University, Chandigarh*

³⁰*Peking University, Beijing*

³¹*Saga University, Saga*

³²*University of Science and Technology of China, Hefei*

³³*Seoul National University, Seoul*

³⁴*Sungkyunkwan University, Suwon*

³⁵*University of Sydney, Sydney NSW*

³⁶*Tata Institute of Fundamental Research, Bombay*

³⁷*Toho University, Funabashi*

³⁸*Tohoku Gakuin University, Tagajo*

³⁹*Tohoku University, Sendai*

⁴⁰*Department of Physics, University of Tokyo, Tokyo*

⁴¹*Tokyo Institute of Technology, Tokyo*

⁴²*Tokyo Metropolitan University, Tokyo*

⁴³*Tokyo University of Agriculture and Technology, Tokyo*

⁴⁴*University of Tsukuba, Tsukuba*

⁴⁵*Virginia Polytechnic Institute and State University, Blacksburg, Virginia 24061*

⁴⁶*Yonsei University, Seoul*

⁴⁷*Princeton University, Princeton, New Jersey 08545*

Abstract

We report the first observation of the decay modes $B^0 \rightarrow D^+D^-$, $B^- \rightarrow D^0D^-$ and $B^- \rightarrow D^0D^{*-}$ based on $152 \times 10^6 B\bar{B}$ events collected at KEKB. The branching fractions of $B^0 \rightarrow D^+D^-$, $B^- \rightarrow D^0D^-$ and $B^- \rightarrow D^0D^{*-}$ are found to be $(3.21 \pm 0.57 \pm 0.48) \times 10^{-4}$, $(5.62 \pm 0.82 \pm 0.65) \times 10^{-4}$ and $(4.59 \pm 0.72 \pm 0.56) \times 10^{-4}$, respectively. Charge asymmetries in the $B^- \rightarrow D^0D^-$ and $B^- \rightarrow D^0D^{*-}$ channels are consistent with zero.

PACS numbers: 13.25.Hw, 11.30 Er

Mixing induced CP -violating asymmetries in $b \rightarrow c\bar{c}s$ decays have been observed at the B factory experiments, Belle and BaBar, at levels consistent with Standard Model (SM) predictions [1]. Cabibbo-suppressed double charm decays (e.g. $B^0 \rightarrow D^{(*)+}D^{(*)-}$) are dominated by $b \rightarrow c\bar{c}d$ tree diagram contributions. Additional penguin contributions with a different weak phase are expected to be small in comparison with tree diagram contributions. Hence, time dependent CP -violating asymmetries in such double charm decays should be nearly equal to those in $B^0 \rightarrow J/\psi K_S$ ($b \rightarrow c\bar{c}s$) type decays. However, a variety of processes beyond the SM can provide additional sources of CP violation [2]. Thus, the $B^0 \rightarrow D^{(*)+}D^{(*)-}$ decay modes can be used to confirm the SM predictions of CP violation [3] or to look for physics beyond the Standard Model.

Signals for the decay modes $B^0 \rightarrow D^{*+}D^{*-}$, $B^0 \rightarrow D^{*+}D^-$ and $B^0 \rightarrow D^+D^{*-}$ have already been observed. Measurements of time dependent CP -violating asymmetry parameters are also available for these modes [4]. While the branching fraction for $B^0 \rightarrow D^+D^-$ is expected to be fairly large, evidence for this decay mode has not yet been reported. Using SU(3) symmetry and the world-average branching fraction [5], $\mathcal{B}(B^0 \rightarrow D^+D^-)$ is estimated to be $\sin^2 \theta_c \times \mathcal{B}(B^0 \rightarrow D_s^+D^-) \simeq (4.0 \pm 1.5) \times 10^{-4}$, where θ_c is the Cabibbo angle.

The decay modes $B^- \rightarrow D^0D^-$ and $B^- \rightarrow D^0D^{*-}$ are expected to be dominated by tree diagrams with some additional contributions from penguin diagrams. Scaling from the well-measured branching fractions for the Cabibbo-favored processes $B^- \rightarrow D^0D_s^-$ and $B^- \rightarrow D^0D_s^{*-}/B^- \rightarrow D^{*0}D_s^-$, one can estimate the branching fractions of these two decay modes to be $(6.5 \pm 2.0) \times 10^{-4}$ and $(5.1 \pm 2.2) \times 10^{-4}$, respectively. Assuming SU(3) symmetry, measurement of these branching fractions will enable better understanding of the penguin processes.

Here, we report the first observation of the decays $B^0 \rightarrow D^+D^-$, $B^- \rightarrow D^0D^-$ and $B^- \rightarrow D^0D^{*-}$. Inclusion of charge conjugate modes is implied throughout this paper. The analysis is based on a 140 fb^{-1} data sample at the $\Upsilon(4S)$ resonance (10.58 GeV) and a 16 fb^{-1} data sample 60 MeV below the $\Upsilon(4S)$ peak (referred to as off-resonance data), collected with the Belle detector [6] at the energy asymmetric e^+e^- collider KEKB [7]. The data sample contains $152 \times 10^6 B\bar{B}$ events. The fractions of neutral and charged B mesons produced in $\Upsilon(4S)$ peak are assumed to be equal.

The Belle detector is a general purpose magnetic spectrometer with a 1.5 T magnetic field provided by a superconducting solenoid. Charged particles are measured using a 50 layer Central Drift Chamber (CDC) and a three layer double sided Silicon Vertex Detector (SVD). Photons are detected in an electromagnetic calorimeter (ECL) consisting of 8736 CsI(Tl) crystals. Exploiting the information acquired from an array of 128 time-of-flight counters (TOF), an array of 1188 silica aerogel Čerenkov threshold counters (ACC) and dE/dx -measurements in the CDC, we derive particle identification (PID) likelihoods $\mathcal{L}_{\pi/K}$. A kaon candidate is identified by a requirement on the likelihood ratio $\mathcal{L}_K/(\mathcal{L}_K + \mathcal{L}_\pi)$ such that the average kaon identification efficiency is $\sim 93\%$ with pion misidentification rate of $\sim 10\%$. Similarly, charged pions are selected with an efficiency of $\sim 95\%$ and kaon misidentification rate of $\sim 10\%$. We select charged pions and kaons that originate from the region $dr < 1 \text{ cm}$ and $|dz| < 4 \text{ cm}$ with respect to the run dependent interaction points (IP), where dr , dz are the distances of closest approach of π/K tracks to the IP in the plane perpendicular to and along the z -axis (the z -axis is defined as passing through the nominal interaction point and antiparallel to the positron beam). All tracks compatible with the electron hypothesis ($\sim 0.2\%$ misidentification rates from pion/kaon) are eliminated. No attempt has been made to

identify muons, which represent a background of about 2.7% to the pion tracks.

Neutral kaons (K_S) are reconstructed via the decay $K_S \rightarrow \pi^+\pi^-$ with no particle identification requirement for daughter pions and the two-pion invariant mass is required to be within $11 \text{ MeV}/c^2$ ($\sim 3.5\sigma$, where σ is the invariant mass resolution of $\pi^+\pi^-$) of the K_S mass. To improve the purity of K_S candidates, we impose K_S momentum-dependent criteria on the impact parameter of the pions, the distance between the closest approaches of the pions along the beam direction, the distance of the $\pi^+\pi^-$ vertex from the interaction point, and the azimuthal angle difference between the direction of $\pi^+\pi^-$ vertex from the IP and the K_S momentum direction. Mass and vertex constrained fits are applied to obtain the 4-momenta of K_S candidates. Neutral pions (π^0) are reconstructed from pairs of isolated ECL clusters (photons) with invariant mass in the window $118 \text{ MeV}/c^2 < M_{\gamma\gamma} < 150 \text{ MeV}/c^2$ ($\sim \pm 3\sigma$). The energy of each photon is required to be greater than 30 MeV in the barrel region, defined as $32^\circ < \theta_\gamma < 128^\circ$, and greater than 50 MeV in the endcap regions, defined as $17^\circ < \theta_\gamma \leq 32^\circ$ or $128^\circ < \theta_\gamma \leq 150^\circ$, where θ_γ denotes the polar angle of the photon. Mass constrained fits are applied to obtain the 4-momenta of π^0 candidates.

Beam gas events are rejected using the requirements $|P_z| < 2 \text{ GeV}/c$ and $0.5 < E_{\text{vis}}/\sqrt{s} < 1.25$, in the $\Upsilon(4S)$ rest frame, where P_z and E_{vis} are the sum of the longitudinal momentum and the energy of all reconstructed particles, respectively, and \sqrt{s} is the sum of the beam energies in the $\Upsilon(4S)$ rest frame. The continuum ($e^+e^- \rightarrow q\bar{q}$, where $q = u, d, s, c$) events are suppressed by requirements on the ratio of the second to the zeroth Fox-Wolfram moments [8], $R_2 < 0.35$.

The D^0 meson is reconstructed through its decay to $K^-\pi^+$, $K^-\pi^+\pi^0$, $K^-\pi^+\pi^+\pi^-$, $K_S\pi^+\pi^-$ and K^+K^- . The D^+ meson is reconstructed through its decay to $K^-\pi^+\pi^+$ and $K^-K^+\pi^+$. Mass and vertex constrained fits are applied to improve the D meson momentum resolution.

The tracks from the D decays are chosen with a criterion, $|dz_i - dz_j| < 2 \text{ cm}$, where $dz_{i(j)}$ is the distance of closest approach of track $i(j)$ to the IP along the z -axis. Large combinatorial backgrounds are removed by requiring that the invariant mass of daughter particles is within 2.5σ from the nominal D -mass, where σ ($\sim 4.5 \text{ MeV}/c^2$), the mass resolution, depends on the decay chain.

D^{*+} candidates are reconstructed by combining the D^0 with a slow charged pion with $dr < 2 \text{ cm}$ and $|dz| < 10 \text{ cm}$ with respect to the D vertex. D^0 mass windows are widened to $\pm 20 \text{ MeV}/c^2$ for the reconstruction of D^{*+} candidates. D^{*+} candidates are required to have a reconstructed mass difference between the D^{*+} and D^0 within $2.0 \text{ MeV}/c^2$ ($\sim 3.0\sigma$) of the nominal mass difference. A kinematic fit with the D^{*+} mass is applied to obtain the 4-momenta of the D^{*+} candidate.

To reduce large combinatorial backgrounds in D^0 decays to $K^-\pi^+\pi^+\pi^-$, a tighter impact parameter requirement, $dr < 0.5 \text{ cm}$, is applied to all four tracks. Note that this is not applied for $D^{*+} \rightarrow D^0(\rightarrow K^-\pi^+\pi^+\pi^-)\pi^+$ signals because this mode has much less background. The $D^0 \rightarrow K^-\pi^+\pi^0$ decay mode is used only for D^{*+} candidates to avoid large backgrounds in D^0 signals in this decay mode.

Combinations of $D\overline{D}^{(*)}$ are used to reconstruct candidate B mesons. $D\overline{D}^{(*)}$ signals are contaminated with background from misidentified D mesons and also combination of two D candidates from opposite B mesons. There are two important kinematic variables to extract signals from these backgrounds, (i) the energy difference, ΔE , between the measured energy

of the candidate event and the beam energy, E_{beam} , in the $\Upsilon(4S)$ rest frame and (ii) the beam energy constrained mass, $M_{\text{bc}} = \sqrt{E_{\text{beam}}^2 - (\sum_i \vec{P}_i)^2}$, where \vec{P}_i are momentum vectors of the primary $D^{(*)}$ candidates. The ΔE distribution is used to extract the signal yield since peaking backgrounds are expected in the M_{bc} distributions. The fit is performed for events where M_{bc} satisfies $5.272 \text{ GeV}/c^2 < M_{\text{bc}} < 5.288 \text{ GeV}/c^2$ and the fit range in ΔE is from -70 MeV to 200 MeV . The restricted range in negative ΔE is chosen to exclude contributions from other B decays, such as $B^0 \rightarrow \overline{D}^0 D^{*0} (D^{*0} \rightarrow D^0 \gamma)$. Selected events contain multiple B candidates with a multiplicity depending on the signal channels, which varies from 1.02 to 1.07. In events with more than one candidate B meson, the candidate with the smallest $\chi^2 (= (\Delta M_{D_1}/\sigma_{M_{D_1}})^2 + (\Delta M_{D_2}/\sigma_{M_{D_2}})^2)$ is chosen, where ΔM_{D_i} is the difference of the reconstructed and nominal mass of D_i , and $\sigma_{M_{D_i}}$ is the resolution in M_{D_i} . In $B^- \rightarrow D^0 D^{*-}$ candidates, a $(\Delta M_{D^{*-}}/\sigma_{M_{D^{*-}}})^2$ term is also added to the χ^2 to choose the best candidate, where $\Delta M_{D^{*-}}$ is the difference between measured and nominal mass difference between D^{*-} and \overline{D}^0 , and $\sigma_{M_{D^{*-}}}$ is the resolution in measured mass difference.

Unbinned extended maximum likelihood fits to ΔE distributions are used to extract the signal yields. The signal shape is modeled as a sum of two Gaussians,

$$F(\Delta E) = A \left\{ \exp \left[-0.5 \left(\frac{\Delta E - \mu}{\sigma} \right)^2 \right] + f_1 \exp \left[-0.5 \left(\frac{\Delta E - \mu}{f_2 \sigma} \right)^2 \right] \right\}$$

which is dominated by a Gaussian of width, $\sigma \sim 6 \text{ MeV}$ and a wider Gaussian, whose width is $\sim 2\text{--}3$ times larger than the main Gaussian function, but whose contribution is only 15%–17% of the main Gaussian function. Backgrounds are modeled with a linear function.

Signal Monte Carlo (MC) is fitted with this function to determine f_1 and f_2 . The fitted values of f_1 and f_2 are 0.051 and 2.48, respectively. The ΔE distribution in data is wider than in MC. The decay channel, $B^- \rightarrow D^0 D_s^-$ is used as a control sample to calculate the scaling factor, $f (= [\sigma_{\text{data}}/\sigma_{\text{MC}}]_{B^- \rightarrow D^0 D_s^-} = 1.08 \pm 0.05)$ of the Gaussian width in data.

To extract signal yields from data, the width of the main Gaussian function is fixed to $\sigma = f \sigma_{\text{MC}}$ and remaining four parameters (parameters A and μ of signal function and two parameters of the linear background function) are determined in the fit.

Signal and backgrounds are studied with Monte Carlo event samples that are generated using the QQ event generator [9]. The response of the Belle detector is simulated by a GEANT3-based program [10]. The simulated events are reconstructed and analysed with the same procedure as is used for the real data. A large generic $B\overline{B}$ MC samples, with a luminosity equivalent to 330 fb^{-1} of data is used to look for peaking backgrounds in ΔE distributions. We have also studied feed across among these signals and from other $B \rightarrow \overline{D}^{(*)} \overline{D}^{(*)}$ decays. Background due to continuum events are studied by analysing the 16 fb^{-1} of off-resonance data and simulated MC events equivalent to $\sim 330 \text{ fb}^{-1}$ of data. No peaking backgrounds are observed in ΔE distributions of these samples. Signal efficiencies in $B^0 \rightarrow D^+ D^-$, $B^- \rightarrow D^0 D^-$ and $B^- \rightarrow D^0 D^{*-}$ decay modes are $11.9 \pm 0.1\%$, $11.1 \pm 0.1\%$ and $4.8 \pm 0.1\%$, respectively.

Figure 1 shows the ΔE distributions in data for the decay modes $B^0 \rightarrow D^+ D^-$, $B^- \rightarrow D^0 D^-$ and $B^- \rightarrow D^0 D^{*-}$. There are clear structures near $\Delta E = 0$. The results of the fits for

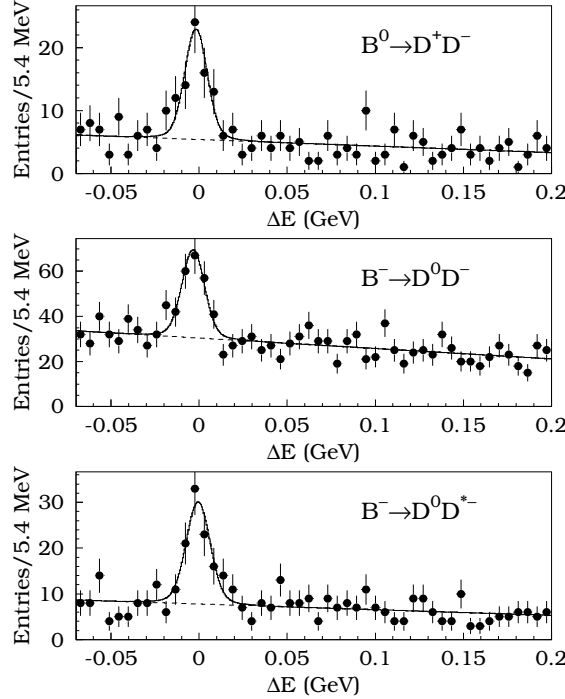


FIG. 1: Fit results of ΔE distributions in data. Points with error bars are the observed events in data, solid lines are the results from the fit and dashed lines represent the background components.

TABLE I: Observed signal yields, statistical significances (σ) and branching fractions.

Channel	N_{obs}	σ	$\mathcal{B} \times 10^4$				
$B^0 \rightarrow D^+ D^-$	54.3	\pm	9.7	7.3	3.21	\pm	0.57
$B^- \rightarrow D^0 D^-$	120.5	\pm	17.6	8.0	5.62	\pm	0.82
$B^- \rightarrow D^0 D^{*-}$	73.6	\pm	11.5	8.2	4.59	\pm	0.72

these decay modes are also shown in these plots. The signal yields obtained from the fits are given in Table I. The statistical significance of the yields, defined as $\sqrt{-2 \ln(\mathcal{L}_0/\mathcal{L}_{\text{max}})}$, is 7.3, 8.0 and 8.2 for the $B^0 \rightarrow D^+ D^-$, $B^- \rightarrow D^0 D^-$ and $B^- \rightarrow D^0 D^{*-}$ channels, respectively, where $\mathcal{L}_0(\mathcal{L}_{\text{max}})$ is the maximum likelihood without (with) the signal contribution. The corresponding ΔE distributions for events in the M_{bc} sideband region ($5.2 \text{ GeV}/c^2 < M_{bc} < 5.26 \text{ GeV}/c^2$) are also checked and they do not show any structure. To check for possible background from modes such as $B \rightarrow DK\pi$, $B \rightarrow DK\pi\pi$ or charmless $B \rightarrow K\pi K(n\pi)$, we also examine the B signal yield for combinations when one of the D candidates has an invariant mass in a sideband outside the nominal D mass window. No significant yield is observed in such combinations.

Branching fractions obtained for these three modes are listed in Table I, where the first error is statistical and the second error is systematic. This is the first measurement of the branching fractions for these decay modes. All results are consistent with the expectation from SU(3) symmetry. As a consistency check, the M_{bc} distributions are also fitted after

constraining $|\Delta E| < 40$ MeV and they show consistent signal yields.

The distribution of the helicity angle for $B^- \rightarrow D^0 D^{*-}$ channel is also studied. The helicity angle, Θ , is defined as the angle between the direction opposite to the B meson and that of the slow pion in the the D^{*-} rest frame. Figure 2 shows the ΔE sideband subtracted (the signal region is defined as $|\Delta E| < 20$ MeV and sideband regions are $50 \text{ MeV} < |\Delta E| < 70 \text{ MeV}$) helicity angle distributions in data and for the MC signal. The data follow a $\cos^2 \Theta$ distribution as expected for a B to pseudoscalar-vector decay.

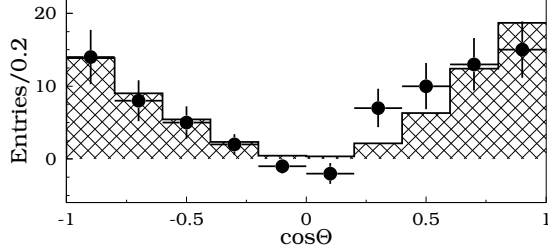


FIG. 2: Background-subtracted distribution of the cosine of the helicity angle in $D^{*-} \rightarrow \overline{D}^0 \pi^-$ decay for $B^- \rightarrow D^0 D^{*-}$ candidates in data (points with error bars) and for $B^- \rightarrow D^0 D^{*-}$ signal MC (hatched histogram).

The systematic uncertainty, shown in Table II, is obtained from a quadratic sum of the uncertainties in (a) the track finding efficiency, ranging from 1% for high momentum tracks to 8% for pions of 80 MeV/ c , estimated from partially reconstructed $D^{*-} \rightarrow \overline{D}^0 (\rightarrow K_S (\rightarrow \pi^+ \pi^-) \pi^+ \pi^-) \pi^-$ events and a track embedding study; (b) the π^0 reconstruction efficiency, estimated from a comparison of $D^0 \rightarrow K^- \pi^+ \pi^0$ yields in data and MC; (c) the K_S selection efficiency, estimated from a comparison of $D^0 \rightarrow K_S \pi^+ \pi^-$ yields in data and MC; (d) K/π selection efficiencies, estimated using $D^{*-} \rightarrow \overline{D}^0 (\rightarrow K^+ \pi^-) \pi^-$ events; (e) The world-average D^0, D^+ and D^{*+} branching fractions [5]; (f) scaling factor for ΔE distributions in data; (g) MC statistics; (h) the total number of $B\overline{B}$ events ($N_{B\overline{B}}$). The systematic error is also studied by (a) varying the ΔE fit ranges within -200 MeV to $+200$ MeV; (b) the choice of the fitting functions; (c) deriving the branching fraction without selection of the best candidate. Systematic uncertainties from the latter three sources are negligible compared to those from the other sources.

Charge asymmetry, $A = (N_- - N_+)/N_+ + N_-)$ in $B^- \rightarrow D^0 D^-$ and $B^- \rightarrow D^0 D^{*-}$ channels is $-0.05 \pm 0.15 \pm 0.05$ and $0.15 \pm 0.15 \pm 0.05$, respectively, where $N_- (N_+)$ is the number of observed events in $B^- (B^+)$ decays. Systematic errors on charge asymmetries are determined from high statistics $B^- \rightarrow D^{(*)0} D_s^{(*)-}$ and $B \rightarrow D^*(n\pi)$ event samples.

In summary, we report first observations of the decays $B^0 \rightarrow D^+ D^-$, $B^- \rightarrow D^0 D^-$ and $B^- \rightarrow D^0 D^{*-}$ using 152 million $B\overline{B}$ events. We measure branching fractions for these three decay modes, which are consistent with the expectation from SU(3) symmetry. Charge asymmetries in the $B^- \rightarrow D^0 D^-$ and $B^- \rightarrow D^0 D^{*-}$ are consistent with zero. We find a statistically significant signal in the $B^0 \rightarrow D^+ D^-$ channel; in the future this mode will be used to perform additional studies of time dependent CP violation in $b \rightarrow c\overline{c}d$ decays.

We thank the KEKB group for the excellent operation of the accelerator, the KEK cryogenics group for the efficient operation of the solenoid, and the KEK computer group and the

TABLE II: Individual contributions of systematic uncertainties (in %).

	D^+D^-	D^0D^-	D^0D^{*-}
Track finding	6.5	7.2	9.1
π^0	-	-	2.0
K_S	-	0.4	1.0
K/π selection	5.5	5.5	5.1
ΔE scale	2.4	2.6	2.2
MC statistics	0.9	1.2	2.0
$N_{B\bar{B}}$	0.5	0.5	0.5
D branching fractions	12.1	6.6	5.3
Total	15.0	11.5	12.1

NII for valuable computing and Super-SINET network support. We acknowledge support from MEXT and JSPS (Japan); ARC and DEST (Australia); NSFC (contract No. 10175071, China); DST (India); the BK21 program of MOEHRD and the CHEP SRC program of KOSEF (Korea); KBN (contract No. 2P03B 01324, Poland); MIST (Russia); MESS (Slovenia); Swiss NSF; NSC and MOE (Taiwan); and DOE (USA).

* on leave from Nova Gorica Polytechnic, Nova Gorica

- [1] Belle Collaboration, K. Abe *et al.*, Phys. Rev. **D66**, 071102(R) (2002), BaBar Collaboration, B. Aubert *et al.*, Phys. Rev. Lett. **89**, 201802 (2002).
- [2] Y. Grossman and M. Worah, Phys. Lett. **B395**, 241 (1997).
- [3] A.I. Sanda and Zhi-zhong Xing, Phys. Rev. **D56**, 341 (1997).
- [4] Belle Collaboration, K. Abe *et al.*, Phys. Rev. Lett. **89**, 122001 (2002), BaBar Collaboration, B. Aubert *et al.*, Phys. Rev. Lett. **89**, 061801 (2002), BaBar Collaboration, B. Aubert *et al.*, Phys. Rev. Lett. **90**, 221801 (2003), Belle Collaboration, T. Aushev *et al.*, Phys. Rev. Lett. **93**, 201802 (2004), Belle Collaboration, H. Miyake *et al.*, Submitted to Phys. Lett. **B**.
- [5] S. Eidelman *et al.*, (Particle Data Group), Phys. Lett. **B592**, 1 (2004).
- [6] Belle Collaboration, A. Abashian *et al.*, Nucl. Instr. Meth. **A479**, 117, (2002).
- [7] S. Kurokawa and E. Kikutani, Nucl. Instr. Meth. **A499**, 1 (2003).
- [8] G. C. Fox and S. Wolfram, Phys. Rev. Lett. **41** (1978) 1581.
- [9] The QQ B meson decay event generator was developed by the CLEO Collaboration, <http://www.lns.cornell.edu/public/CLEO/soft/QQ>
- [10] CERN Program Library Long Writeup, W5013, CERN, 1993.